Bicelle to Vesicle Transition of a Binary Phospholipid Mixture Guided by Controlled Local Lipid Compositions: A Molecular Dynamics Simulation Study

Kenichiro Koshiyama[*1], *Masaki Taneo*[2], *Taiki Shigematsu*[3], *and Shigeo Wada*[2]

[1]Graduate School of Technology, Industrial and Social Sciences, Tokushima University, Tokushima, 770-8506, Japan

[2]Graduate School of Engineering Science, Osaka University, Toyonaka, 560-8531, Japan

[3]Global Center for Medical Engineering and Informatics, Osaka University, 2-2 Yamadaoka, Suita, 565-0871, Japan

AUTHOR INFORMATION

E-mail: koshiyama@tokushima-u.ac.jp

Abstract. An essential step of nanoliposome formation in an aqueous lipid solution is the transition from discoidal lipid aggregate (bicelle) to vesicle. We here investigate the bicelle-vesicle transition of a binary lipid mixture of saturated and unsaturated phosphatidylcholine by performing nonequilibrium molecular dynamics simulations with the coarse-grained representation of di-palmitoyl-phosphatidyl-choline (DPPC) and di-linoleoyl-phosphatidyl-choline (DLiPC). When DPPC molecules of a stable DPPC bicelle are randomly replaced to DLiPC molecules, the transition occurs for higher apparent DLiPC concentrations. On the other hand, when the DPPC molecules only in the core region of the bicelle are replaced, the transition occurs even for lower apparent DLiPC concentrations. For the bicelle where the head and tail layers are, respectively, pure DPPC and DLiPC monolayers, the side of DLiPC monolayer becomes the concave surface of bending bicelle. Controlling the local lipid compositions in binary lipid bicelle has the potential to determine the success of vesicle formation and the direction of bicelle bending. Our findings help explain nanoliposome formation with sonication and give useful information for controlling encapsulation efficiencies of nanoliposomes.

Introduction

Liposomes are vesicular structures composed of lipid bilayers, which can entrap molecules of various sizes. Nano-sized liposomes, i.e., nanoliposomes, have biocompatibility and biodegradability because of their nanoscale characteristics, and the application as vehicles to deliver exogenous molecules has been widely attempted in cosmetics, food technology, agriculture, and nanomedicine[1–5]. However, they are known to have some limitations such as stability, reproducibility, or molecular encapsulation efficiency. A fundamental understanding of nanoliposome formation is required for the development of nanoliposome applications.

The transition from discoidal lipid aggregate (bicelle) to vesicle has been recognized as an essential step of liposome formation[6–8]. Qualitatively, the transition can be explained by a balance between bending and edge energies with approximated shapes and macroscopic mechanical properties of a single lipid aggregate. Molecular-scale simulations, such as molecular dynamics (MD)[9–14] and Brownian dynamics simulations[15], have complemented and improved the simple qualitative picture with detailed information about lipid molecular dynamics. For example, molecular simulations of nanoliposome formation from randomly distributed lipid in water have revealed the aggregation process of lipids[9–14] and the effects of temperature or lipid compositions on detailed vesicle structure[13,14]. Previously, we investigated nanoliposome formation under sonication with coarse-grained (CG) MD simulations[11]. Sonication is one of the standard methods to prepare nanoliposomes[4,5,16–19], which utilizes ultrasound cavitation phenomenon to reduce liposomal sizes. Our study revealed that, after collapsing a lipid-coated nanobubble, bicelle with folds of various amplitudes forms, and temporal bicelle structure affects the transition and detailed vesicle structure[11]. These molecular simulations suggest that lipid molecular dynamics and distributions in nanoscale lipid aggregate is an important factor governing the transition.

Despite extensive molecular simulation studies on liposome formation for pure lipid systems[9–12], little is known for multi-lipid systems. To our knowledge, only the binary lipid systems composed of di-palmitoyl-phosphatidyl-choline(DPPC) and di-palmitoyl-phosphatidyl-ethanolamine or DPPC and di-linoleoyl-phosphatidyl-choline (DLiPC) have been used in nanoliposome simulation studies[13,14]. In our previous study[11], we investigated the effects of saturation of lipid tails on the liposome formation from a lipid-coated nanobubble composed of DPPC or DLiPC, but it was limited to single lipid systems. Experimentally, binary or ternary lipid systems have been used for liposome or bicelle studies, and it is speculated that the lipid composition of multi-lipid bicelle affects both static and dynamics behavior[20–23]. Furthermore, liposomes composed of multi-lipid mixtures are available in more practical applications[1]. Consequently, it is a principal research object to understand the effects of lipid compositions and dynamics on nanoliposome formation in lipid mixtures.

In this study, we investigate the bicelle-vesicle transition of a binary lipid mixture composed of phosphatidylcholine (PC) lipid molecules with saturated and unsaturated tails in aqueous solution by CG MD simulations. We clarify the effects of the apparent and local concentrations of unsaturated lipid molecules on the transition in lipid mixture systems at the molecular scales with DPPC/DLiPC lipid mixtures. We numerically demonstrate that forcibly-concentrated unsaturated lipid molecules in the core region of a stable bicelle facilitate the bicelle-vesicle transition. Also, with biased-initial bicelle configurations where the head and tail layers are, respectively, saturated- and unsaturated- lipid monolayers, the side of unsaturated lipid layer becomes the concave surface of bending bicelle. Our findings help explain nanoliposome formation with sonication and may give useful information for controlling encapsulation efficiencies of nanoliposome.

Methods

Nonequilibrium MD Simulation of DPPC/DLiPC Mixtures

We consider the bicelle-vesicle transition of a binary-lipid mixture composed of DPPC and DLiPC molecules in water. To model molecules, we use the MARTINI force field[24], which is a CG model suitable for semi-quantitative evaluation of lipid aggregation dynamics with MD simulation while reducing computational cost. The MARTINI DPPC and DLiPC lipid molecules have the same CG headgroup, but the CG tail of DLiPC is developed accounting for the flexible character of the polyunsaturated linoleyl tail and the polarizable nature of the double bond[14,24,25]. Consistently to analyze effects of local unsaturated lipid compositions on the transition, we regard the MARTINI DPPC and DLiPC as representative saturated and unsaturated PC lipid molecules with similar tail length, respectively. The initial structure is a single disk-like lipid aggregate (bicelle) composed of 600 DPPC molecules in 78,501 MARTINI water beads with periodic boundary conditions. The DPPC bicelle is stable at 1 bar and 323 K as shown in the previous study[11]. In order to investigate the effects of the local lipid composition on the bicelle-vesicle transition, the DPPC molecules of the bicelle are replaced to DLiPC molecules at various apparent DLiPC concentrations. The apparent DLiPC concentration C is defined as $C = N_{\mathrm{u}} / N_{\mathrm{l}}$, where N_{u} is the number of DLiPC molecules and N_{l} is the total number of lipid molecules. We set the lipid selection method as the random selection, the core selection, the head and tail selection, and their combination (see below). For the head and tail selection, we develop a selection algorithm with gyration tensor[26] consistently to divide lipid molecules into the head or tail monolayer of bicelle. To this end, we first calculate the gyration tensor of bicelle and obtain the eigenvalues and eigenvectors. As the eigenvector of the smallest eigenvalue is a normal vector of the bicelle surface,

we can allocate lipid molecules to head or tail of bicelle by the inner product of the normal vector and the position vector of each phospholipid molecule with respect to the center of bicelle.

After replacing lipid molecules in the bicelle, to relax the lipid systems, we perform short constant volume and temperature and constant pressure and temperature MD simulations for at least 0.4 μs. The leap-frog algorithm is used to integrate the equation of motions, and the time step is 20 fs. The velocity-rescale method[27] is used to relax and maintain the temperature at 323 K with the coupling constant of 1.0 ps. The Berendsen method[28] is used to relax and keep the pressure at 1 bar with the time constant of 2.0 ps. Because interpretations of nonequilibrium MD simulations of lipid systems require statistical treatment[29,30], we perform MD simulations started from at least ten different initial configurations for each condition. All MD simulations are performed with GROMACS 4.6.7[31–33] and with common MARTINI CG parameters. For visualization, Visual Molecular Dynamics (VMD)[34] is used. Note that, considering the current improvement of MD simulation algorithms and parameter-verification for the MARTINI force field, we verified the effects of them on the results with GROMACS 5.1.5 and newer MARTINI CG parameters[35], although the selection of them have minor effects on the outcomes.

Evaluation of Bending Modulus

The bending modulus k_c of a DPPC/DLiPC mixture is estimated based on the Fourier transformation of DPPC/DLiPC bilayer undulations[36]. The bilayer systems are composed of 8,192 lipid molecules and 392,928 MARTINI water beads with periodic boundary conditions for various apparent DLiPC concentrations. The bilayer systems equilibrate in the MD simulation at constant temperature (323 K) and constant pressure (1 bar) for at least 0.6 μs. The bending modulus k_c is obtained by using the following relationship, $S_u(q) = k_B T / a k_c q^4$, where $S_u(q)$ is the fluctuation

spectra of the bilayer surface with respect to the magnitude of wave vector q, a is the area per lipid, k_B is Boltzmann's constant, and T is the temperature, under the assumption of vanishing bilayer surface tension and small q. The wave vector is defined as $\mathbf{q} = \left(q_x, q_y\right) = 2\pi\left(n/L_x, m/L_y\right)$ with n, m = 0, ±1, ±2, ±3…, the projected area of the bilayer $L_x L_y$, and $q = |\mathbf{q}| = \sqrt{q_x^2 + q_y^2}$. We fit the above function to the spectra under 0.7 nm^{-1} with the largest box length $L_{max} = 50$ nm. In order to compare the qualitative trend, k_cs for various DLiPC concentrations are normalized with respect to the value for pure DPPC. Note that k_c for a pure DPPC bilayer obtained here is $\sim 15 \times 10^{-20}$ J, which is larger than those obtained with previous undulation analysis, but close to the values obtained with the recent orientation analysis and the shape fluctuation analysis by experiments[37]. Because our bilayer system (8,192 lipid molecules) is larger than previous bilayer systems[37] (typically, 640~6,400 lipid molecules), we believe that our results with the undulation analysis are reasonable to fit the above relationship to the spectra of the bilayer undulations.

Evaluation of Line Tension

The line tension γ of a DPPC/DLiPC mixture is estimated based on the pressure balance of bilayer ribbon systems[38]. The base system of bilayer ribbon is composed of 512 DPPC molecules and 40,987 MARTINI water beads with periodic boundary conditions. The simulation box size is $21.56 \times 12.56 \times 21.56$ nm^3 in the x, y, and z directions, respectively, where the y-direction is the axial direction of the ribbon. The bilayer ribbon system equilibrates in the MD simulation at constant temperature (323 K), constant pressure in the x- and z-directions (1 bar), and constant length of the simulation box in the y-direction for 0.5 μs. After the equilibration, the DPPC molecules of the ribbon are randomly selected and replaced to DLiPC molecules at various

apparent concentrations. The binary-lipid bilayer ribbon systems are further equilibrated for 2.5 μs, and the trajectories during the final 1.5 μs are used in the analyses. The line tension γ is calculated using $\gamma = \left(\left(P_{xx} + P_{zz} \right) / 2 - P_{yy} \right) l_x l_y / 2$, where P_{ii} and l_i are the pressure tensor and the simulation box length in the *i*-direction (*i* = *x*, *y*, or *z*), respectively. The results for various apparent concentrations are normalized with respect to the value for pure DPPC ribbon system (50.6 pN), which is close to the value reported previously[39].

Results

Bicelle to Vesicle Transition of DPPC/DLiPC Mixture

During relaxation MD simulations of DPPC/DLiPC bicelle prepared with the random selection method, lipid molecules rearrange in bicelle. The transition from bicelle to vesicle occurs via bowl-like shape (Fig. 1 (A)) depending on the apparent DLiPC concentration *C*. Figure 1 (B) shows the probability to the vesicle formation *P*, which is defined as $P = N_{\mathrm{V}} / N_{\mathrm{T}}$, where N_{V} is the number of trials of vesicle formation during relaxation and N_{T} is the total number of trials. Pure DPPC bicelle remains stable ($P = 0$ at $C = 0$), whereas pure DLiPC bicelle spontaneously transitions to vesicular shape ($P = 1$ at $C = 1$), as confirmed in the previous study[11]. For $C > 0.6$, P increases and reaches 1.0 at $C = 0.9$. This result suggests that the critical concentration for the transition of a DPPC/DLiPC mixture can be found for $C > 0.6$.

The macroscopic theory of vesicle formation predicts that a balance between bending and edge energies determines the shape of lipid aggregate[6,7]. Considering the constant number of lipid molecules ($= 600$) in the bicelle system, the bending modulus k_{c} and line tension γ of a DPPC/DLiPC mixture would be essential factors for the energy balance. We estimate k_{c} and γ

based on the Fourier transformation of DPPC/DLiPC bilayer undulations[36] and the pressure balance of DPPC/DLiPC ribbon system[38], respectively. k_c of DPPC/DLiPC bilayer decreases with the apparent DLiPC concentration of bilayer system C_b (Fig. 1 (C)). Likewise, γ of DPPC/DLiPC ribbon decreases with the apparent concentration of the ribbon system C_r, but becomes almost unchanged for $C_r \geq 0.4$ (Fig. 1 (D)). Because the DLiPC concentration per edge length of the ribbon becomes saturated around $C_r =\sim 0.4$ (Fig. S1), it is suggested that γ of DPPC/DLiPC bicelle depends not on the apparent concentration but the DLiPC concentration per edge length as in DPPC/DLiPC ribbon systems.

In binary DPPC/DLiPC bicelle, when started from random DLiPC distributions (Fig. 2 (A), left), DLiPC molecules rapidly cap the edge of bicelle to reduce the edge energy, while concentrating DPPC molecules in the core region of bicelle (Fig. 2 (A), right). Figure 2 (B) shows the relationships between the core DLiPC concentration C_C, which is calculated for the lipid molecules within 2.0 nm lateral distance in the bicelle plane from the center of mass of bicelle, and the apparent DLiPC concentration *C*. The relationship exhibits low DLiPC concentration in the core region of DPPC/DLiPC bicelle, i.e., the high DLiPC concentration in the edge region. Such partitioning of lipid molecules in bicelle can be confirmed in other studies, although it depends on the compositions of lipid mixtures[21,40].

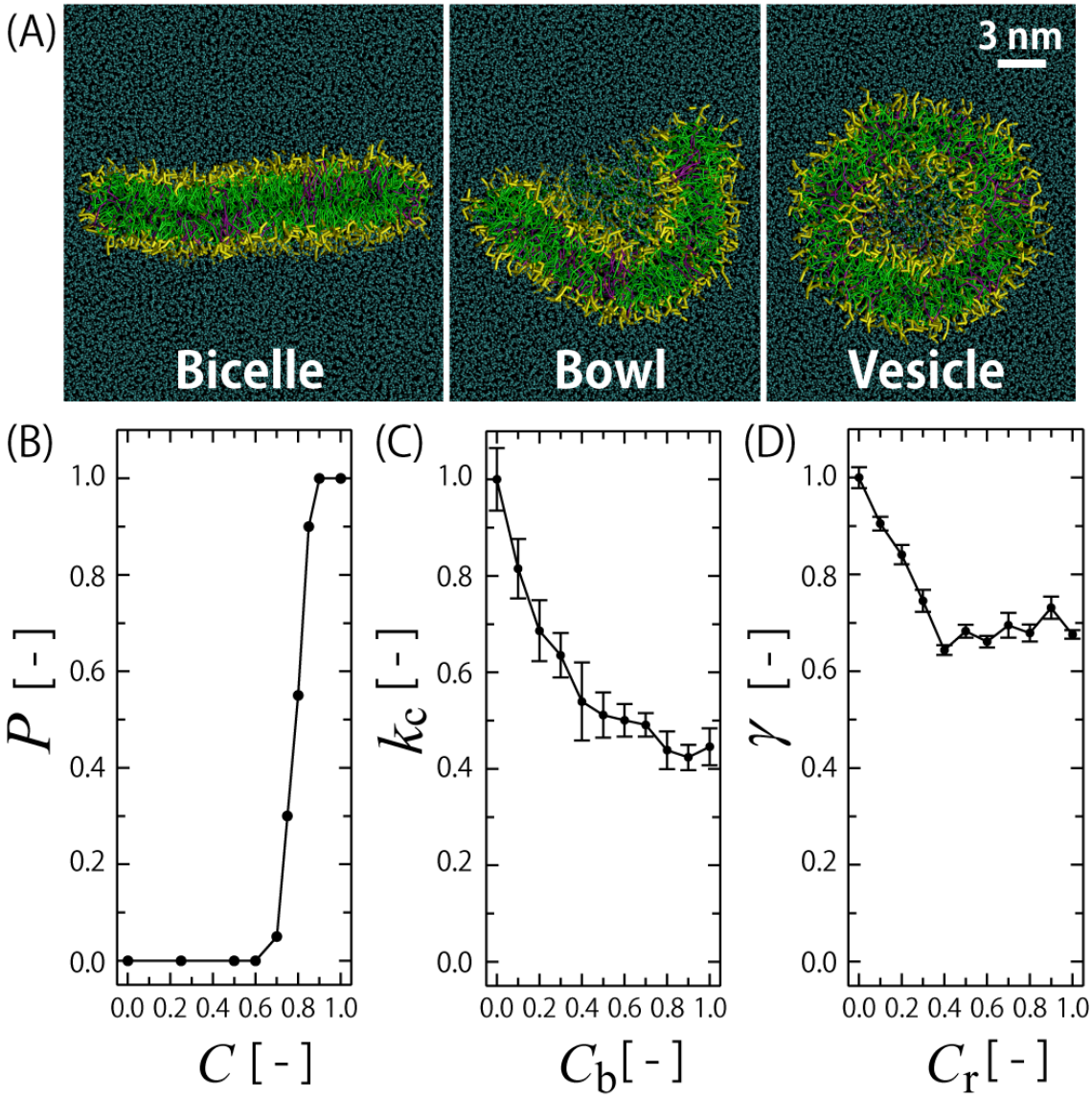

Figure 1. Representative snapshots (cutaways) of the transition from bicelle to vesicle via bowl-like shape for $C = 0.85$ (A), the probabilities of vesicle formation from the DPPC/DLiPC bicelle P for the apparent concentration C (B), the bending modulus of the DPPC/DLiPC bilayer k_c for the concentration of bilayer C_b (C), and the line tension of the DPPC/DLiPC ribbon γ for the concentration of ribbon C_r (D). The PC headgroups are shown in yellow, the DLiPC tails in green, the DPPC tails in purple, and water in cyan. Note that k_c and γ are normalized with respect to those for the pure DPPC system. The error bars represent the standard errors calculated by comparing 50 ns and 250 ns blocks for k_c and γ, respectively.

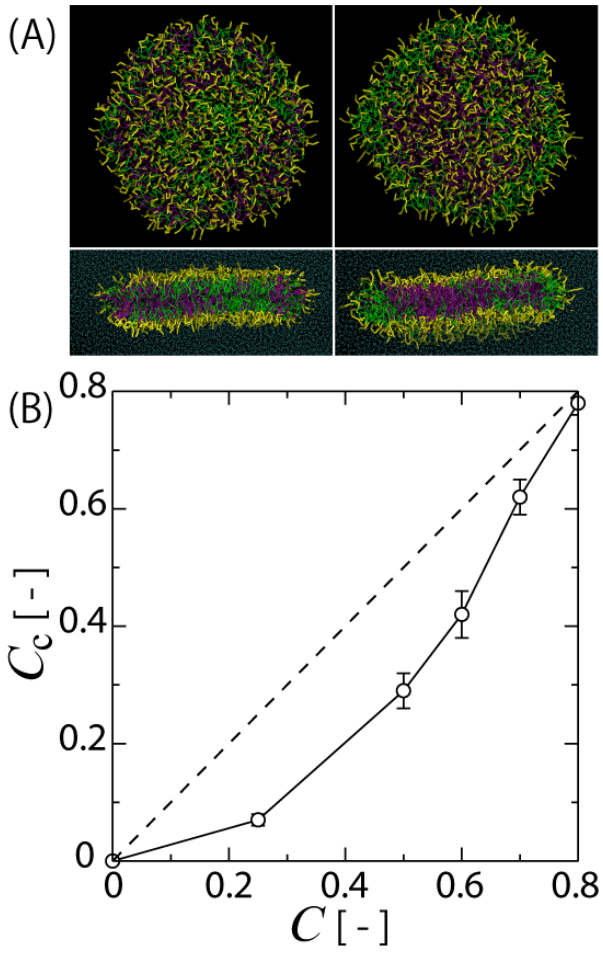

Figure 2. Representative snapshots (top and side views) of a DPPC/DLiPC bicelle before (left) and after (right) relaxation from a random DLiPC distribution for $C = 0.50$ (A) and the relationship between the core and apparent concentrations of DLiPC molecules in DPPC/DLiPC bicelle (B). Water molecules in top views are not shown for clarity. The error bars in Fig. 2 (B) shows the standard deviation.

Effects of Local Lipid Compositions

Deducing from the transition associated with the spatial distribution of DLiPC molecules in bicelle (see above), the initial spatial distribution of DLiPC molecules in DPPC/DLiPC bicelle could be involved in the transition. Numerically to confirm this, we perform relaxation MD simulations from biased-initial configurations of binary lipid mixture. Specifically, as initial

configurations, we replace DPPC to DLiPC molecules only in the core region of pure DPPC bicelle (Fig. 3 (A), inset). During relaxation, the bowl-like shape forms immediately from the biased-initial configuration (Fig. 3 (B), upper and middle), followed by vesicle formation even for the lower apparent concentrations $C \geq 0.15$ (Fig. 3 (A)). However, once the bowl-like shape fails the transition to vesicle, DLiPC molecules spread from the core region and cap the edge, resulted in stable bicelle structure (see, e.g., Fig.2 (A)).

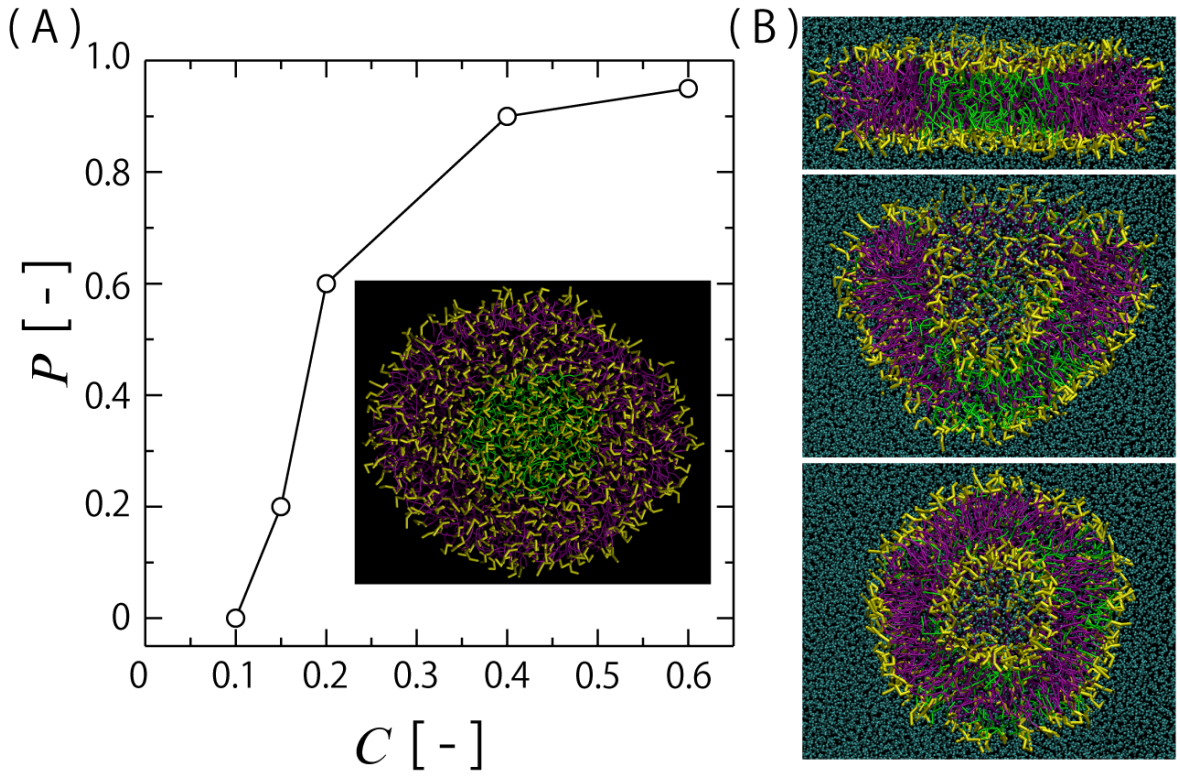

Figure 3. The probabilities of vesicle formation from the biased initial configuration of DPPC/DLiPC bicelle (inset) for various apparent concentrations (A) and representative snapshots of the vesicle formation via bowl-like shape for $C = 0.20$ (B).

Transition from Bicelle to Bowl-like shape

For the hydrophilic small molecular encapsulation[41], the transition from bicelle to bowl-like shape should be an essential process because solutions beside a concave surface of bending bicelle are primarily taken into the inside of a nanoliposome (Fig. S2). According to the macroscopic theory[7], the direction of spontaneous bending of bicelle to bowl-like shape is primarily statistical in pure lipid bicelle. Considering the difference of mechanical properties between pure DPPC and DLiPC aggregate (e.g., Fig. 1 (C)), the spatial DLiPC distribution in DPPC/DLiPC bicelle may affect the direction of the bicelle bending. We numerically investigate the effect of DLiPC distribution in the bicelle on the bending direction by performing relaxation MD simulations from a biased-initial configuration, where the head and tail monolayers of bicelle are composed of a pure DLiPC and DPPC monolayer, respectively (Fig. 4 (A), upper). The side of DLiPC monolayer always becomes the concave surface of bowl-like shape (Fig. 4 (A), middle), which might relate to the inverted cone-shaped characteristic of DLiPC[14]. However, the bowl-like shape recovers to bicelle in due course, and the bicelle structure becomes stable (Fig. 4 (A), lower) because the apparent concentration of the bicelle is 0.5 (see Fig. 1 (B)), and DLiPC molecules rapidly cap the bicelle edge (Fig. 4 (A), lower).

Higher DLiPC concentration in the core region of bicelle enhances the transition to vesicle (Fig. 3). We further replace DPPC molecules in the core region of the side of pure DPPC monolayer to DLiPC molecules in the head and tail initial configuration (Fig.4 (B), inset). As expected, the transition to vesicle can be confirmed (Fig. 4 (B)), while the direction of bending, i.e., the concave surface, is the side of DLiPC monolayer in the biased bicelle.

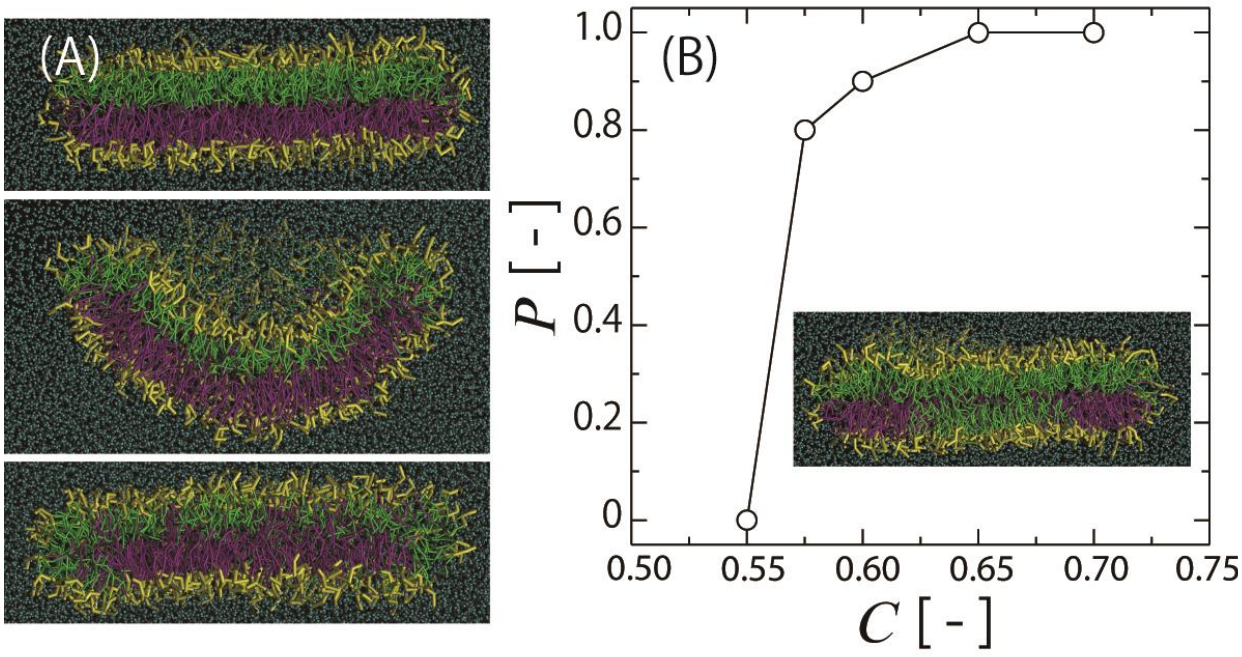

Figure 4. Representative snapshots of bicelle bending from the head and tail initial configuration (see text) (A) and the probabilities of vesicle formation from the biased initial configuration of DPPC/DLiPC bicelle (Fig. 4 (B) inset).

Discussion

During relaxation of DPPC/DLiPC bicelle, we found the transition to vesicle generally occurs for higher apparent DLiPC concentrations, $C > 0.6$ (Fig. 1 (B)). This result can be explained by the conventional energetic consideration[6,7], where a balance between bending and edge energies determines the stable shape of lipid aggregate. For lower *C*, the edge energy gain is dominant by decreasing in γ due to higher DLiPC concentration in the edge region (Fig. 1 (D) and Fig. 2 (B)), and, hence, bicelle structure is stable. On the other hand, for higher *C*, the bending energy gain becomes dominant because of the saturated edge-energy gain while the lowering of k_c (see Fig. 1 (C) and (D)). Accordingly, vesicle transition should be favorable for higher C ($P >\sim 0.5$ for

$C > 0.8$ in Fig. 1 (B)), where the core DLiPC concentration C_C closes to the apparent concentration C (Fig. 2 (B)). Toward the quantitative estimation, other factors, e.g., local area per lipids, bicelle shape approximation, and saddle splay modulus should be investigated. Moreover, because the resulted DPPC/DLiPC vesicles have radii of ~5 nm (Fig. 1 (A) and Fig. S3), it might be needed to consider the curvature-dependent elastic moduli to evaluate the free energy of small unilamellar vesicles with lipid mixture more precisely[42,43].

When the DPPC molecules only in the core region of a stable DPPC bicelle are replaced to DLiPC, the transition occurs even for lower apparent DLiPC concentrations (Fig. 3). The procedure might lower the local bending modulus while keeping the line tension to be higher value temporally (Fig. 1 (C) and (D)), which is favorable for the transition to vesicle according to the energetic consideration[6,7]. Also, vesicles of various sizes can be formed for the vesicles from the biased initial configurations (Fig. S3). This finding proves that the initial DLiPC distribution in DPPC/DLiPC bicelle is an essential factor to form a vesicle, especially for lower DLiPC concentration. Under sonication, ultrasound cavitation creates and collapses lipid-coated nanobubbles[4,18], and, just after the collapse, bicelle with complicated structure forms[11], which implies that sonication can temporarily induce inhomogeneous lipid distribution in bicelle. Experimentally, multi-lipid vesicle prepared with sonication shows bi-modal size distribution at the nanoscales depending on the sonication time[4]. Although the typical sonicated vesicles have radii of ~15 nm with considerable variation[44] and composed of more complexed lipid compositions, the temporary inhomogeneous lipid distribution due to collapsing bubbles seems to be a part of reasons why the sonication is favorable to decreases multi-lipid vesicles to nanosize and yields bi-modal size distributions of vesicles in a mixture of lipids.

Our simulations have also revealed that controlling the local lipid compositions in binary lipid bicelle has the potential to determine the direction of bicelle bending (Fig. 4). Recent lipid experiments have suggested that plasma-induced lipid oxidation techniques have the potential to induce the local chemical modification of lipid tails[45], which may relate to structural changes of lipid aggregate at the molecular scale[46]. Moreover, the recent simulation study on oxidized lipid bilayer[47] suggests the possibility to control the level of oxidation via the introduction of protective molecules. Although further investigations are required, the techniques to control local lipid compositions in bicelle may be favorable to encapsulate small hydrophilic molecules combined with various methods for liposome preparation[41,48].

In the binary DPPC/DLiPC bicelle, we observed the migration of DLiPC to the edge of bicelle (Fig. 2). Based on the rigid shape model for single lipid systems[49], both the cylindrical shaped DPPC and the inverted-cone shaped DLiPC should be unfavorable to residing in the edge region. Because of the flexible tails of DLiPC[14], the DLiPC might be more adaptable to the edge, at least, for DPPC/DLiPC bicelle. Also, we speculate that the less hydrophobic nature of the double bonds of polyunsaturated linoleyl tails may affect the DLiPC migration too. For example, because the hydrophobic tails would be partly exposed to water at the edge of bicelle (Fig. S4), the unsaturated-tail/water interface, i.e., less hydrophobic interface, could be favorable for binary saturated/unsaturated lipid system. Accordingly, the line tension decreases with the DLiPC concentration of DPPC/DLiPC mixture (Fig. 1 (D)). Strictly, each CG lipid model corresponds to a range of atomistic structure[25], and it might be required systematically to investigate packing in multi-lipid systems with all-atom or united atom lipid representation, although it is beyond the scope of this work.

Conclusions

We have investigated the bicelle-vesicle transition of a DPPC/DLiPC mixture in aqueous solution by CG MD simulations. We have demonstrated that the critical value of the apparent concentration of DLiPC for the transition of the DPPC/DLiPC bicelle can be found in the concentrations larger than 0.6, and the value significantly decreases when DLiPC lipid molecules are forcibly concentrated only in the core region of bicelle. Also, the local DLiPC concentrations of a DPPC/DLiPC bicelle can control the spontaneous bending direction of DPPC/DLiPC bicelle and the success of vesicle formation. The inhomogeneous lipid distribution in bicelle, which may be induced by collapsing bubbles, may relate to the bi-modal size distribution of multi-lipid vesicles with sonication at the molecular scale. Our findings suggest that controlling the local lipid compositions in a binary lipid bicelle has a potential to determine the success of vesicle formation and the direction of bicelle bending, which may be useful information to control encapsulation efficiency of nanoliposomes. Numerical information of lipid molecular dynamics associated with nanoliposome formation promotes further experimental studies on liposome formation in multi-lipid mixtures and the development of nanoliposome formation methods for further applications.

AUTHOR INFORMATION

Corresponding author: Kenichiro Koshiyama, Tel: +81 88 656 9187; E-mail: koshiyama@tokushima-u.ac.jp

Notes

The authors declare no competing financial interests.

Acknowledgments

We hereby acknowledge the Grants received from JSPS (JP15K01284, JP17K13033).

Supporting Information Available: Local concentration of DLiPC in DPPC/DLiPC ribbon, Representative snapshots of the bicelle-vesicle transition, Structure of small DPPC/DLiPC vesicles, Enlarged side view of the bicelle edge.

References

(1) Jesorka, A.; Orwar, O. Liposomes: Technologies and Analytical Applications. *Annu. Rev. Anal. Chem.* **2008**, *1*, 801–832.

(2) Immordino, L.; Dosio, F.; Cattel, L.; Immordino, M. L.; Dosio, F.; Cattel, L. Stealth Liposomes: Review of the Basic Science, Rationale, and Clinical Applications, Existing and Potential. *Int. J. Nanomedicine* **2006**, *1*, 297–315.

(3) Hallaj-Nezhadi, S.; Hassan, M. Nanoliposome-Based Antibacterial Drug Delivery. *Drug Deliv.* **2015**, *22*, 581–589.

(4) Woodbury, D. J.; Richardson, E. S.; Grigg, A. W.; Welling, R. D.; Knudson, B. H. Reducing Liposome Size with Ultrasound: Bimodal Size Distributions. *J. Liposome Res.* **2006**, *16*, 57–80.

(5) Mozafari, M. R. Nanoliposomes: Preparation and Analysis. In *Methods in Molecular biology*; Volkmar Weissig, Ed.; Humana Press: New York, NY, 2010.

(6) Helfrich, W. The Size of Bilayer Vesicles Generated by Sonication. *Phys. Lett.* **1974**, *50A*, 115–116.

(7) Fromherz, P. Lipid-Vesicle Structure: Size Control by Edge-Active Agents. *Chem. Phys. Lett.* **1983**, *94*, 259–266.

(8) Lasic, D. D. A General Model of Vesicle Formation. *J. Theor. Biol.* **1987**, *124*, 35–41.

(9) De Vries, A. H.; Mark, A. E.; Marrink, S. J. Molecular Dynamics Simulation of the Spontaneous Formation of a Small DPPC Vesicle in Water in Atomistic Detail. *J. Am. Chem. Soc.* **2004**, *126*, 4488–4489.

(10) Marrink, S. J.; de Vries, A. H.; Tieleman, D. P. Lipids on the Move: Simulations of Membrane Pores, Domains, Stalks and Curves. *Biochim. Biophys. Acta-Biomembranes* **2009**, *1788*, 149–168.

(11) Koshiyama, K.; Wada, S. Collapse of a Lipid-Coated Nanobubble and Subsequent Liposome Formation. *Sci. Rep.* **2016**, *6*, 28164.

(12) Shinoda, W.; DeVane, R.; Klein, M. L. Zwitterionic Lipid Assemblies: Molecular Dynamics Studies of Monolayers, Bilayers, and Vesicles Using a New Coarse Grain Force Field. *J. Phys. Chem. B* **2010**, *114*, 6836–6849.

(13) Chng, C.-P. Effect of Simulation Temperature on Phospholipid Bilayer–vesicle Transition Studied by Coarse-Grained Molecular Dynamics Simulations. *Soft Matter* **2013**, *9*, 7294.

(14) Risselada, H. J.; Marrink, S. J. Curvature Effects on Lipid Packing and Dynamics in Liposomes Revealed by Coarse Grained Molecular Dynamics Simulations. *Phys. Chem. Chem. Phys.* **2009**, *11*, 2056–2067.

(15) Noguchi, H.; Gompper, G. Dynamics of Vesicle Self-Assembly and Dissolution. *J. Chem. Phys.* **2006**, *125*, 1–13.

(16) Shen, K. C.; Kakumanu, S.; Beckett, C. D.; Laugharn, J. A. Use of Adaptive Focused Acoustics™ Ultrasound in Controlling Liposome Formation. *Ultrason. Sonochem.* **2015**, *27*, 638–645.

(17) Silva, R.; Ferreira, H.; Little, C.; Cavaco-Paulo, A. Effect of Ultrasound Parameters for Unilamellar Liposome Preparation. *Ultrason. Sonochem.* **2010**, *17*, 628–632.

(18) Richardson, E. S.; Pitt, W. G.; Woodbury, D. J. The Role of Cavitation in Liposome Formation. *Biophys. J.* **2007**, *93*, 4100–4107.

(19) Szoka, F.; Papahadjopoulos, D. Comparative Properties and Methods of Preparation of Lipid Vesicles (Liposomes). *Annu. Rev. Biophys. Bioeng.* **1980**, *9*, 467–508.

(20) Feigenson, G. W. Phase Behavior of Lipid Mixtures. *Nat. Chem. Biol.* **2006**, *2*, 560–563.

(21) Cho, H. S.; Dominick, J. L.; Spence, M. M. Lipid Domains in Bicelles Containing Unsaturated Lipids and Cholesterol. *J. Phys. Chem. B* **2010**, *114*, 9238–9245.

(22) Triba, M. N.; Devaux, P. F.; Warschawski, D. E. Effects of Lipid Chain Length and Unsaturation on Bicelles Stability. A Phosphorus NMR Study. *Biophys. J.* **2006**, *91*, 1357–1367.

(23) Katsaras, J.; Harroun, T. A.; Pencer, J.; Nieh, M.-P. "Bicellar" Lipid Mixtures as Used in Biochemical and Biophysical Studies. *Naturwissenschaften* **2005**, *92*, 355–366.

(24) Marrink, S. J.; Risselada, H. J.; Yefimov, S.; Tieleman, D. P.; de Vries, A. H. The MARTINI Force Field: Coarse Grained Model for Biomolecular Simulations. *J. Phys. Chem. B* **2007**, *111*, 7812–7824.

(25) Wassenaar, T. A.; Ingólfsson, H. I.; Böckmann, R. A.; Tieleman, D. P.; Marrink, S. J. Computational Lipidomics with Insane: A Versatile Tool for Generating Custom Membranes for Molecular Simulations. *J. Chem. Theory Comput.* **2015**, *11*, 2144–2155.

(26) Theodorou, D. N.; Suter, U. W. Shape of Unperturbed Linear Polymers: Polypropylene. *Macromolecules* **1985**, *18*, 1206–1214.

(27) Bussi, G.; Donadio, D.; Parrinello, M. Canonical Sampling through Velocity Rescaling. *J. Chem. Phys.* **2007**, *126*, 014101.

(28) Berendsen, H. J. C.; Postma, J. P. M.; van Gunsteren, W. F.; DiNola, a; Haak, J. R. Molecular Dynamics with Coupling to an External Bath. *J. Chem. Phys.* **1984**, *81*, 3684–3690.

(29) Koshiyama, K.; Kodama, T.; Yano, T.; Fujikawa, S. Structural Change in Lipid Bilayers and Water Penetration Induced by Shock Waves: Molecular Dynamics Simulations. *Biophys. J.* **2006**, *91*, 2198–2205.

(30) Koshiyama, K.; Yano, T.; Kodama, T. Self-Organization of a Stable Pore Structure in a Phospholipid Bilayer. *Phys. Rev. Lett.* **2010**, *105*, 018105.

(31) Hess, B.; Kutzner, C.; van der Spoel, D.; Lindahl, E. GROMACS 4: Algorithms for Highly Efficient, Load-Balanced, and Scalable Molecular Simulation. *J. Chem. Theory Comput.* **2008**, *4*, 435–447.

(32) Berendsen, H. J. C.; Vanderspoel, D.; Vandrunen, R. Gromacs - a Message-Passing Parallel Molecular-Dynamics Implementation. *Comput. Phys. Commun.* **1995**, *91*, 43–56.

(33) Pronk, S.; Pall, S.; Schulz, R.; Larsson, P.; Bjelkmar, P.; Apostolov, R.; Shirts, M. R.; Smith, J. C.; Kasson, P. M.; van der Spoel, D.; et al. GROMACS 4.5: A High-Throughput and Highly Parallel Open Source Molecular Simulation Toolkit. *Bioinformatics* **2013**, *29*, 845–854.

(34) Humphrey, W.; Dalke, A.; Schulten, K. VMD: Visual Molecular Dynamics. *J. Mol. Graph. Model.* **1996**, *14*, 33–38.

(35) de Jong, D. H.; Baoukina, S.; Ingólfsson, H. I.; Marrink, S. J. Martini Straight: Boosting Performance Using a Shorter Cutoff and GPUs. *Comput. Phys. Commun.* **2016**, *199*, 1–7.

(36) Brandt, E. G.; Braun, A. R.; Sachs, J. N.; Nagle, J. F.; Edholm, O. Interpretation of Fluctuation Spectra in Lipid Bilayer Simulations. *Biophys. J.* **2011**, *100*, 2104–2111.

(37) Chaurasia, A. K.; Rukangu, A. M.; Philen, M. K.; Seidel, G. D.; Freeman, E. C. Evaluation of Bending Modulus of Lipid Bilayers Using Undulation and Orientation Analysis. *Phys. Rev. E* **2018**, *97*, 1–12.

(38) Jiang, F. Y.; Bouret, Y.; Kindt, J. T. Molecular Dynamics Simulations of the Lipid Bilayer Edge. *Biophys. J.* **2004**, *87*, 182–192.

(39) Jiang, Y.; Kindt, J. T. Simulations of Edge Behavior in a Mixed-Lipid Bilayer: Fluctuation Analysis. *J. Chem. Phys.* **2007**, *126*, 045105.

(40) De Joannis, J.; Jiang, F. Y.; Kindt, J. T. Coarse-Grained Model Simulation of Mixed-Lipid Systems: Composition and Line Tension of a Stabilized Bilayer Edge. *Langmuir* **2006**, *22*, 998–1005.

(41) Eloy, J. O.; Claro de Souza, M.; Petrilli, R.; Barcellos, J. P. A.; Lee, R. J.; Marchetti, J. M. Liposomes as Carriers of Hydrophilic Small Molecule Drugs: Strategies to Enhance Encapsulation and Delivery. *Colloids Surfaces B Biointerfaces* **2014**, *123*, 345–363.

(42) Nakamura, T.; Shinoda, W. Method of Evaluating Curvature-Dependent Elastic Parameters for Small Unilamellar Vesicles Using Molecular Dynamics Trajectory. *J. Chem. Phys.* **2013**, *138*, 124903.

(43) Shinoda, W.; Nakamura, T.; Nielsen, S. O. Free Energy Analysis of Vesicle-to-Bicelle Transformation. *Soft Matter* **2011**, *7*, 9012–9020.

(44) Tenchov, B. G.; Yanev, T. K.; Tihova, M. G.; Koynova, R. D. A Probability Concept about Size Distributions of Sonicated Lipid Vesicles. *Biochim. Biophys. Acta* **1985**, *816*, 122–130.

(45) Ki, S. H.; Park, J. K.; Sung, C.; Lee, C. B.; Uhm, H.; Choi, E. H.; Baik, K. Y. Artificial Vesicles as an Animal Cell Model for the Study of Biological Application of Non-Thermal Plasma. *J. Phys. D. Appl. Phys.* **2016**, *49*, 085401.

(46) Boonnoy, P.; Jarerattanachat, V.; Karttunen, M.; Wong-Ekkabut, J. Bilayer Deformation, Pores, and Micellation Induced by Oxidized Lipids. *J. Phys. Chem. Lett.* **2015**, *6*, 4884–4888.

(47) Boonnoy, P.; Karttunen, M.; Wong-Ekkabut, J. Does α-Tocopherol Flip-Flop Help to Protect Membranes Against Oxidation? *J. Phys. Chem. B* **2018**, *122*, 10362–10370.

(48) Patil, Y. P.; Jadhav, S. Novel Methods for Liposome Preparation. *Chem. Phys. Lipids* **2014**, *177*, 8–18.

(49) Israelachvili, J. N. *Intermolecular and Surface Forces*, 3rd ed.; Academic Press: Burlington, MA, 2011.

TOC Graphic

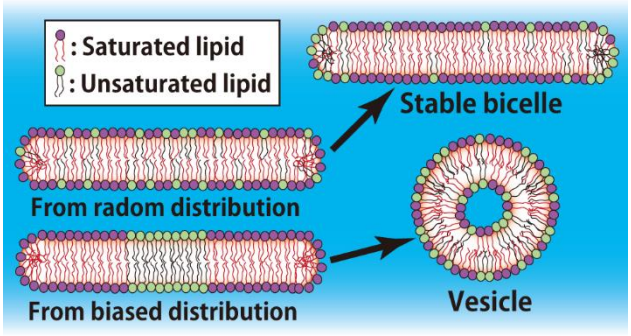
: Saturated lipid
: Unsaturated lipid
Stable bicelle
From radom distribution
From biased distribution
Vesicle

Supporting Information

Bicelle to Vesicle Transition of a Binary Phospholipid Mixture Guided by Controlled Local Lipid Compositions: A Molecular Dynamics Simulation Study

Kenichiro Koshiyama[*1], *Masaki Taneo*[2], *Taiki Shigematsu*[3], *and Shigeo Wada*[2]

[1]Graduate School of Technology, Industrial and Social Sciences, Tokushima University, Tokushima, 770-8506, Japan

[2]Graduate School of Engineering Science, Osaka University, Toyonaka, 560-8531, Japan

[3]Global Center for Medical Engineering and Informatics, Osaka University, 2-2 Yamadaoka, Suita, 565-0871, Japan

AUTHOR INFORMATION

E-mail: koshiyama@tokushima-u.ac.jp

Local Concentration of DLiPC in DPPC/DLiPC Ribbon

To calculate the spatial distribution of DLiPC and DPPC molecules in DPPC/DLiPC ribbon, we define the local axis (ξ) on the ribbon as the eigenvector of the largest eigenvalue of the gyration tensor on the *x*-*z* plain. We calculate the local DLiPC concentration as a function of the distance from the center of mass (COM) of bilayer ribbon along the ξ-axis. The core region of the bilayer ribbon is defined as where the distance from COM along the ξ-axis is within 1 nm and the edge region as where the distance from the bilayer edge is within 1 nm. The position of the lipid molecule is represented by that of the phosphate bead in the head group of the lipid molecule. Fig. S1 shows the DLiPC concentrations in the core and the edge regions as a function of the apparent concentration C_r. As with the bicelle (Fig. 2(B)), the DLiPC concentration in the core of the bilayer ribbon is lower than the apparent concentration C_r. With increasing C_r, the DLiPC concentration in the edge increases and becomes saturated around C_r = ~0.4.

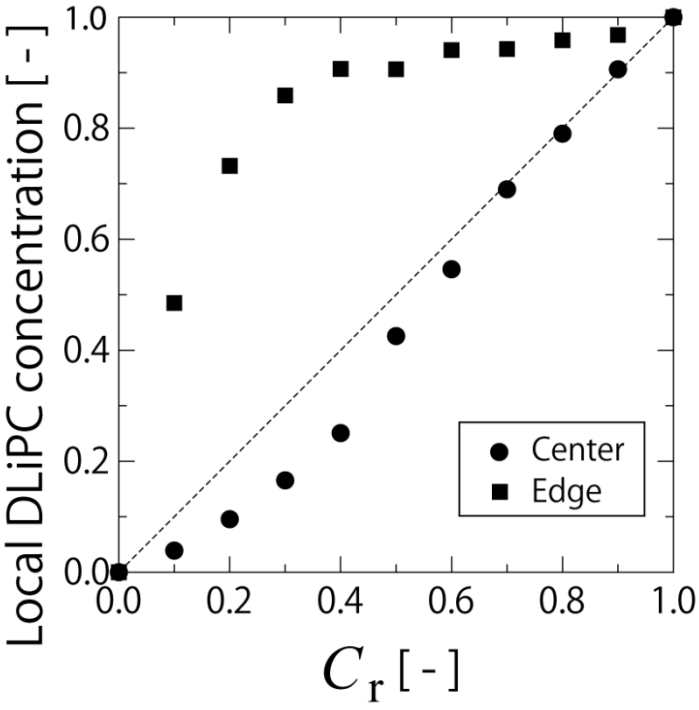

Figure S1. The relationship between the local DLiPC concentrations in the core and edge regions and the apparent DLiPC concentration of the bilayer ribbon.

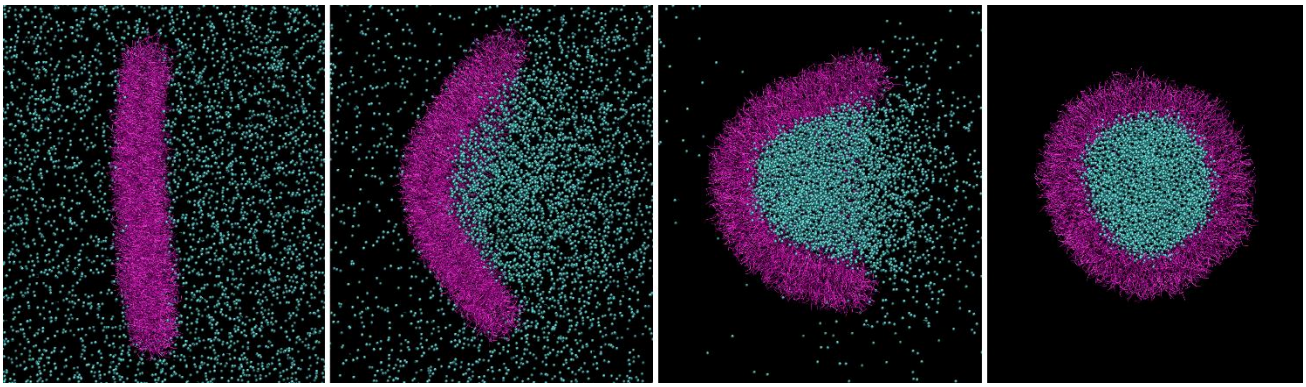

Figure S2. Representative snapshots of the bicelle-vesicle transition of a DPPC lipid aggregate. The lipid (DPPC) molecules are shown in violet and the CG water beads that are enclosed when vesicle forms are shown in cyan. Other water beads are not shown.

Structure of small DPPC/DLiPC vesicles

To investigate the structure of DPPC/DLiPC vesicles for 600 lipid systems, we analyzed the radius of gyration tensor R_g as a measure of vesicle sizes and the inner/outer lipid ratio $R_{\text{io}} = N_{\text{in}} / N_{\text{out}}$, where N_{in} and N_{out} are the number of lipids of the inner and outer monolayers, respectively[1] (Fig. S3). R_g ranges from ~4.5 to ~5.0 nm, and the number of lipids in the inner monolayer is smaller than that of the outer monolayer ($R_{\text{io}} =\sim 0.4$) due to significant differences in curvatures between inner and outer monolayers (e.g., Fig. 1(A)). R_{io} increases with R_g, and the results are confirmed for single lipid vesicles[1]. Furthermore, we analyzed the inner/outer DLiPC concentration ratio $R_{\text{io-DLiPC}} = \left(N_{\text{in-DLiPC}} / N_{\text{in}}\right) / \left(N_{\text{out-DLiPC}} / N_{\text{out}}\right)$, where $N_{\text{in-DLiPC}}$ and $N_{\text{out-DLiPC}}$ are the number of DLiPC of the inner and outer monolayers, respectively (Fig. S3). The vesicles generated from biased initial configurations (Figs. 3 and 4) have a higher DLiPC concentration in the inner monolayer with large variations ($R_{\text{io-DLiPC}} > 1.0$). On the other hand, the DLiPC concentration is similar between the inner and outer monolayers for the vesicles from random initial configurations ($R_{\text{io-DLiPC}} =\sim 1.0$). A

minor enrichment of DLiPC in the inner monolayer of a vesicle can be found for the DPPC/DLiPC vesicle composed of 2,528 lipids with $C = 0.50$ [2].

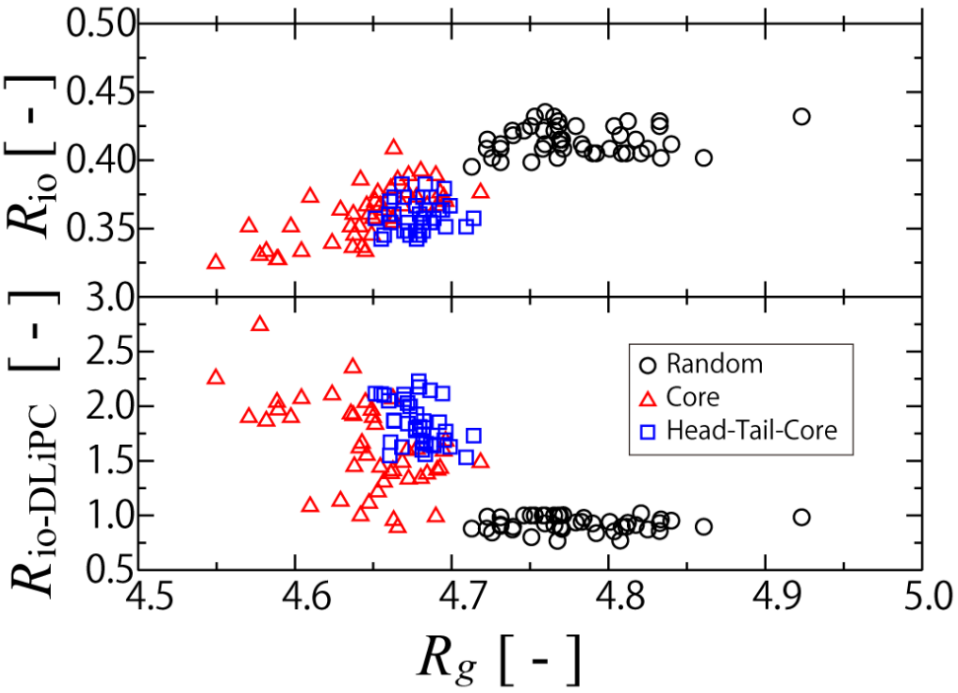

Figure S3. Relationships between R_{io} and R_g (upper) and between $R_{io\text{-}DLiPC}$ and R_g (lower). The black circles show the results for the vesicles from the random configurations, the red triangles from the core configurations, and the blue squares from the head-tail with core configurations.

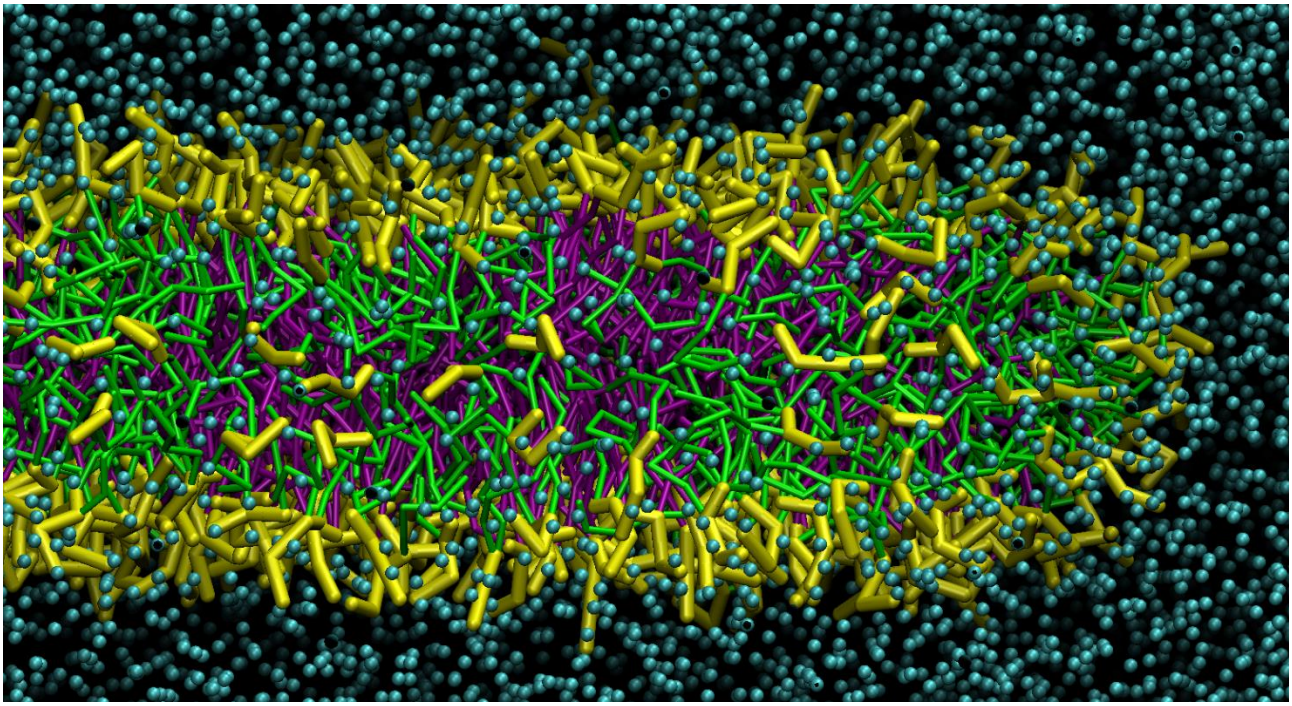

Figure S4. An enlarged side view of the edge of a DPPC/DLiPC bicelle for $C = 0.50$. The number of CG water beads are reduced for clarity.

References

(1) Koshiyama, K.; Wada, S. Collapse of a Lipid-Coated Nanobubble and Subsequent Liposome Formation. *Sci. Rep.* **2016**, *6*, 28164.

(2) Risselada, H. J.; Marrink, S. J. Curvature Effects on Lipid Packing and Dynamics in Liposomes Revealed by Coarse Grained Molecular Dynamics Simulations. *Phys. Chem. Chem. Phys.* **2009**, *11*, 2056–2067.